European Journal of Chemistry

Journal webpage: www.eurjchem.com

Synthesis, structural characterization and biological properties of Cu(II), Ni(II), Mn(II), Zn(II) and VO(II) complexes of tetradentate Schiff bases

Subramanian Vedanayaki [1,*] and Poomalai Jayaseelan [2]

[1] *Department of Chemistry, Kandaswami Kandar's College, Paramathi Velur, Tamilnadu, 638182, India*
[2] *Chemical Division, Mettur Thermal Power Station, Mettur Dam, Tamilnadu, 636406, India*

** Corresponding author at: Department of Chemistry, Kandaswami Kandar's College, Paramathi Velur, Tamilnadu, 638182, India. Tel.: +91.4268.220255. Fax: +91.4268.220255. E-mail address: varshuvishal@gmail.com (S. Vedanayaki).*

ARTICLE INFORMATION

DOI: 10.5155/eurjchem.7.3.368-374.1443

Received: 28 April 2016
Received in revised form: 25 June 2016
Accepted: 02 July 2016
Published online: 30 September 2016
Printed: 30 September 2016

KEYWORDS

Dioxime
Binuclear
Schiff base
DNA binding
DNA cleavage
Antimicrobial activity

ABSTRACT

New binucleating Cu(II), Ni(II), Mn(II), Zn(II) and VO(II) complexes of the prepared ligands with N_4 donor were synthesized. The ligands are obtained by the condensation of *para*-phenylenediamine with diacetylmonoxime and benzilmonoxime. The synthesized ligands and their metal complexes were characterized by elemental analysis and various spectroscopic techniques. The Cu(II), Ni(II) complexes were square planar, VO(II) complex was square pyramidal, whereas Mn(II), Zn(II) complexes were of tedrahedral geometry. Both the ligands and their metal complexes were screened for their antibacterial and antifungal activities by minimum inhibitory concentration method. The results showed that the metal complexes were found to be more active than free ligand. The DNA binding capacities of all the complexes were analyzed by using UV absorption spectra. The DNA cleaving capacities of all complexes were analyzed by agarose gel electrophoresis method against pBR322 DNA.

Cite this: *Eur. J. Chem.* **2016**, *7(3)*, 368-374

1. Introduction

The Schiff base metal complexes have wide range of applications such as, material chemistry, analytical chemistry, catalysis, corrosion and drug delivery [1-7]. Due to presence of hard nitrogen, oxygen and soft sulphur atoms, the Schiff base ligands are easily coordinate with various transition metals. The different co-ordination environment of transition metal complexes offers a great scope for designing species that are suitable to bind and cleave the DNA via oxidative and hydrolytic mechanism. Furthermore, the DNA binding ability of metal complexes has been studied during the past several decades, because it can be used as anticancer drugs and DNA structural probes [8-12]. The factors such as planarity of ligands, coordination geometry and flexible valence are the root causes of binding modes of DNA and in antimicrobial activity, nature of metal ion, hydrophilicity, lipophilicity and coordination sites also have considerable influence on activity. The design and development of potential therapeutic agents, particularly those designed to target nucleic acids site can lead to new approaches to novel therapeutic agents for cancer and antimicrobial activities [13-16].

Due to the importance of Schiff base and its metal complexes in biological fields, we herein report on the synthesis, characterization metal(II) complexes with dioxime ligands. Also, the biological studies of free ligands and its complexes are discussed.

2. Experimental

2.1. Instrumentation

The IR spectra of the samples were recorded on a Perkin-Elmer 783 spectrophotometer in 4000-400 cm^{-1} range using KBr pellet. The UV-Vis spectra were recorded on an INFRA UV-Vis IR-513C spectrophotometer. The elemental analysis was recorded by using thermo Finnegan instrument in Indian Institute of Technology Bombay. The metal concentrations were determined by using Atomic Absorption Spectrometer. The molar conductance of the complexes in DMF (1×10^{-3} M) solution was measured at 27±3 °C with an Elico model conductivity meter. The melting points were determined by Buchi 530 apparatus. ^1H and ^{13}C NMR were recorded in DMSO-d_6 on AV-III 400 (L) in Indian Institute of Science, Bangalore, India. The X-band ESR spectra of the complexes were recorded at room temperature in Indian Institute of Technology, Mumbai, India using tetracyanoethylene as the *g*-marker. Magnetic susceptibility measurements of the complexes were

ISSN 2153-2249 (Print) / ISSN 2153-2257 (Online)
http://dx.doi.org/10.5155/eurjchem.7.3.368-374.1443

carried out by a Guoy balance using copper sulfate as the calibrant.

2.2. Materials and methods

All chemicals and solvents were of reagent grade and were used as received; the metal salts such as copper, nickel, manganese, zinc perchlorates and vanadium(IV) oxide sulfate were purchased from Sigma Aldrich and were used without further purification.

2.2.1. Synthesis of the Schiff base ligand 1

p-Phenylenediamine (1 mM) in 30 mL of absolute ethanol was added to a solution of diacetylmonoxime (2 mM) in 25 mL of absolute ethanol taken in a 100 mL round bottomed flask. The contents were refluxed for about 2 hours; a deep red colored precipitate was formed. The product was filtered, washed with cold ethanol and dried in vacuum desiccator (Scheme 1).

(2E, 2'E, 3E, 3'E)-3, 3'-(1, 4-phenylene-bis(azanylidene))bis (butane-2-one)dioxime (**L1**): Color: Deep red. Yield: 82%. M.p.: 242-244 °C. FT-IR (KBr, ν, cm^{-1}): 3250 (OH), 1620 (C=N), 1432 (N=O). UV/Vis (DMF, λ_{max}, nm): 240, 330. ^{1}H NMR (400 Hz, DMSO-d_6, δ, ppm): 1.90 (m, 6H, CH_3), 2.60 (m, 6H, CH_3), 7.80-8.50 (m, 4H, Ar-H), 11.20 (s, 2H, N-OH). ^{13}C NMR (100 Hz, DMSO-d_6, δ, ppm): 156.18 (2C, C=NOH), 164.69(2C, C=N), 146-138 (4C, Ar-C), 15.19 (2C, CH_3). Λ_m ($ohm^{-1}\cdot cm^2\cdot mol^{-1}$): 9.0. Anal. calcd. for $C_{14}H_{18}N_4O_2$: C, 61.30; H, 6.61; N, 20.42. Found: C, 61.29; H, 6.57; N, 20.40%.

2.2.2. Synthesis of the Schiff base ligand 2

p-Phenylenediamine (1 mM) in 30 mL of absolute ethanol was added to a solution of benzilmonoxime (2 mM) in 25 mL of absolute ethanol taken in a 100 mL round bottomed flask. The contents were refluxed for about 2 hours; a deep red colored precipitate was formed. The product was filtered, washed with cold ethanol and dried in vacuum desiccator (Scheme 2).

(1E, 'E, 2E, 2'E)-2, 2'-(1, 4-phenylene-bis(azanylylidene)bis (1,2-diphenylethane-1-one)dioxime (**L2**): Color: Deep red. Yield: 80%. M.p.: 250-252 °C. FT-IR (KBr, ν, cm^{-1}): 3264 (OH), 1601 (C=N), 1444 (N=O). UV/Vis (DMF, λ_{max}, nm): 250, 340. ^{1}H NMR (400 Hz, DMSO-d_6, δ, ppm): 7.30-7.80 (m, 24H, Ar-H), 11.74 (s, 2H, N-OH). ^{13}C NMR (100 Hz, DMSO-d_6, δ, ppm): 154.63 (2C, C=NOH), 195.20(2C, C=N), 134-125 (4C, Ar-C). Λ_m ($ohm^{-1}\cdot cm^2\cdot mol^{-1}$): 10. Anal. calcd. for $C_{34}H_{26}N_4O_2$: C, 78.14; H, 5.01; N, 10.72. Found: C, 78.40; H, 4.93; N, 10.84%.

2.2.3. Synthesis of the Schiff base metal complexes

The solid chelates were prepared by mixing a hot ethanolic solution of metal(II) salts with the Schiff bases sufficient to form 1:1 (M:L) complexes. The reaction mixture was refluxed for 1 hour on a water bath. The solid chelates were filtered off and washed several times with ethanol and second distilled water until the filtrate becomes colorless. The obtained complexes were kept in vacuum desiccators (Scheme 1 and 2).

$[Cu_2(C_{14}H_{18}N_4O_2)_2]4ClO_4$: Color: Green powder. Yield: 80%. M.p.: 272-274 °C. FT-IR (KBr, ν, cm^{-1}): 3350 (OH), 1609 (C=N), 1510 (N=O), 460 (M-N), 1092 (ClO_4^-). UV/Vis (DMF, λ_{max}, nm): 254, 390, 545. Λ_m ($ohm^{-1}\cdot cm^2\cdot mol^{-1}$): 280. μ_{eff} (B.M.): 1.75 (298 K). Anal. calcd. for $[Cu_2(C_{14}H_{18}N_4O_2)_2]4ClO_4$: C, 31.33; H, 3.38; N, 10.44; M, 11.84. Found: C, 31.28; H, 3.31; N, 10.40; M, 11.81%.

$[Ni_2(C_{14}H_{18}N_4O_2)_2]4ClO_4$: Color: Greenish yellow powder. Yield: 78%. M.p.: 280-282 °C. FT-IR (KBr, ν, cm^{-1}): 3340 (OH), 1616 (C=N), 1436 (N=O), 465 (M-N), 1092 (ClO_4^-). UV/Vis (DMF, λ_{max}, nm): 255, 380, 515. Λ_m ($ohm^{-1}\cdot cm^2\cdot mol^{-1}$): 270. μ_{eff} (B.M.): Diamagnetic. Anal. calcd. for $[Ni_2(C_{14}H_{18}N_4O_2)_2]4ClO_4$: C, 31.61; H, 3.41; N, 10.53; M, 11.03. Found: C, 31.58; H, 3.34; N, 10.55; M, 11.00%.

$[Mn_2(C_{14}H_{18}N_4O_2)_2]4ClO_4$: Color: Dark green powder. Yield: 75%. M.p.: 276-278 °C. FT-IR (KBr, ν, cm^{-1}): 3325 (OH), 1622 (C=N), 1433 (N=O), 465 (M-N), 1087 (ClO_4^-). UV/Vis (DMF, λ_{max}, nm): 255, 395, 430. Λ_m ($ohm^{-1}\cdot cm^2\cdot mol^{-1}$): 275. μ_{eff} (B.M.): 5.24 (298 K). Anal. calcd. for $[Mn_2(C_{14}H_{18}N_4O_2)_2]4ClO_4$: C, 31.84; H, 3.44; N, 10.61; M, 10.40. Found: C, 31.80; H, 3.42; N, 10.59; M, 10.47%.

$[Zn_2(C_{14}H_{18}N_4O_2)_2]4ClO_4$: Color: Pale yellow powder. Yield: 76%. M.p.: 265-267 °C. FT-IR (KBr, ν, cm^{-1}): 3335 (OH), 1609 (C=N), 1512 (N=O), 470 (M-N), 1085 (ClO_4^-). UV/Vis (DMF, λ_{max}, nm): 255, 390. Λ_m ($ohm^{-1}\cdot cm^2\cdot mol^{-1}$): 270. μ_{eff} (B.M.): Diamagnetic. Anal. calcd. for $[Zn_2(C_{14}H_{18}N_4O_2)_2]4ClO_4$: C, 31.22; H, 3.37; N, 10.40; M, 12.14. Found: C, 31.22; H, 3.36; N, 10.46; M, 12.25%.

$[(VO)_2(C_{14}H_{18}N_4O_2)_2]2SO_4^{2-}$: Color: Dark green powder. Yield: 72%. M.p.: 283-285 °C. FT-IR (KBr, ν, cm^{-1}): 3330 (OH), 1614 (C=N), 1475 (N=O), 463 (M-N), 1035 (SO_4^-), 962 (VO^{2-}). UV/Vis (DMF, λ_{max}, nm): 250, 385, 535. Λ_m ($ohm^{-1}\cdot cm^2\cdot mol^{-1}$): 270. μ_{eff} (B.M.): 1.77 (298 K). Anal. calcd. for $[(VO)_2(C_{14}H_{18}N_4O_2)_2]2SO_4^{2-}$: C, 38.45; H, 4.15; N, 12.81; M, 11.65. Found: C, 38.40; H, 4.13; N, 12.88; M, 11.70%.

$[Cu_2(C_{34}H_{26}N_4O_2)_2]4ClO_4$: Color: Green powder. Yield: 85%. M.p.: 275-277 °C. FT-IR (KBr, ν, cm^{-1}): 3407 (OH), 1598 (C=N), 1449 (N=O), 455 (M-N), 1086 (ClO_4^-). UV/Vis (DMF, λ_{max}, nm): 256, 395, 540. Λ_m ($ohm^{-1}\cdot cm^2\cdot mol^{-1}$): 285. μ_{eff} (B.M.): 1.76 (298 K). Anal. calcd. for $[Cu_2(C_{34}H_{26}N_4O_2)_2]4ClO_4$: C, 52.02; H, 3.34; N, 7.14; M, 8.09. Found: C, 51.92; H, 3.33; N, 7.71; M, 8.12%.

$[Ni_2(C_{34}H_{26}N_4O_2)_2]4ClO_4$: Color: Greenish yellow powder. Yield: 80%. M.p.: 282-284 °C. FT-IR (KBr, ν, cm^{-1}): 3410 (OH), 1597 (C=N), 1446 (N=O), 460 (M-N), 1086 (ClO_4^-). UV/Vis (DMF, λ_{max}, nm): 255, 390, 520. Λ_m ($ohm^{-1}\cdot cm^2\cdot mol^{-1}$): 273. μ_{eff} (B.M.): Diamagnetic. Anal. calcd. for $[Ni_2(C_{34}H_{26}N_4O_2)_2]4ClO_4$: C, 52.34; H, 3.36; N, 7.18; M, 7.52. Found: C, 52.32; H, 3.37; N, 7.15; M, 7.50%.

$[Mn_2(C_{34}H_{26}N_4O_2)_2]4ClO_4$: Color: Dark green powder. Yield: 78%. M.p.: 279-281 °C. FT-IR (KBr, ν, cm^{-1}): 3365 (OH), 1597 (C=N), 1446 (N=O), 472 (M-N), 1087 (ClO_4^-). UV/Vis (DMF, λ_{max}, nm): 255, 385. Λ_m ($ohm^{-1}\cdot cm^2\cdot mol^{-1}$): 280. μ_{eff} (B.M.): 5.22 (298 K). Anal. calcd. for $[Mn_2(C_{34}H_{26}N_4O_2)_2]4ClO_4$: C, 52.60; H, 3.38; N, 7.22; M, 7.08. Found: C, 52.60; H, 3.32; N, 7.26; M, 7.13%.

$[Zn_2(C_{34}H_{26}N_4O_2)_2]4ClO_4$: Color: Pale yellow powder. Yield: 76%. M.p.: 268-270 °C. FT-IR (KBr, ν, cm^{-1}): 3323 (OH), 1599 (C=N), 1445 (N=O), 47 8(M-N), 1087 (ClO_4^-). UV/Vis (DMF, λ_{max}, nm): 250, 390. Λ_m ($ohm^{-1}\cdot cm^2\cdot mol^{-1}$): 278. μ_{eff} (B.M.): Diamagnetic. Anal. calcd. for $[Zn_2(C_{34}H_{26}N_4O_2)_2]4ClO_4$: C, 51.90; H, 3.31; N, 7.12; M, 8.31. Found: C, 51.82; H, 3.36; N, 7.15; M, 8.35%.

$[(VO)_2(C_{34}H_{26}N_4O_2)_2]2SO_4^{2-}$: Color: Dark green powder. Yield: 83%. M.p.: 285-287 °C. FT-IR (KBr, ν, cm^{-1}): 3356 (OH), 1593 (C=N), 1447 (N=O), 465 (M-N), 1030 (SO_4^-), 950 (VO^{2-}). UV/Vis (DMF, λ_{max}, nm): 255, 380, 530. Λ_m ($ohm^{-1}\cdot cm^2\cdot mol^{-1}$): 170. μ_{eff} (B.M.): 1.79 (298 K). Anal. calcd. for $C_{68}H_{52}N_8O_{14}S_2V_2$: C, 59.56; H, 3.82; N, 8.17; M, 7.43. Found: C, 59.53; H, 3.42; N, 8.20; M, 7.45%.

2.3. Antimicrobial activity

The free ligands and metal complexes were screened for their antimicrobial activities against the bacteria *Bacillus subtilis, Staphylococcus aureus, Escherichia coli, K. pneumoniae* and fungus *Aspergillus niger* by the disc diffusion method. One day prior to the experiment, the bacterial and fungal cultures were inoculated in nutrient broth (inoculation medium) and incubated overnight at 37 °C. Inoculation medium containing 24 h grown culture was added aseptically to the nutrient medium and mixed thoroughly to get uniform distribution.

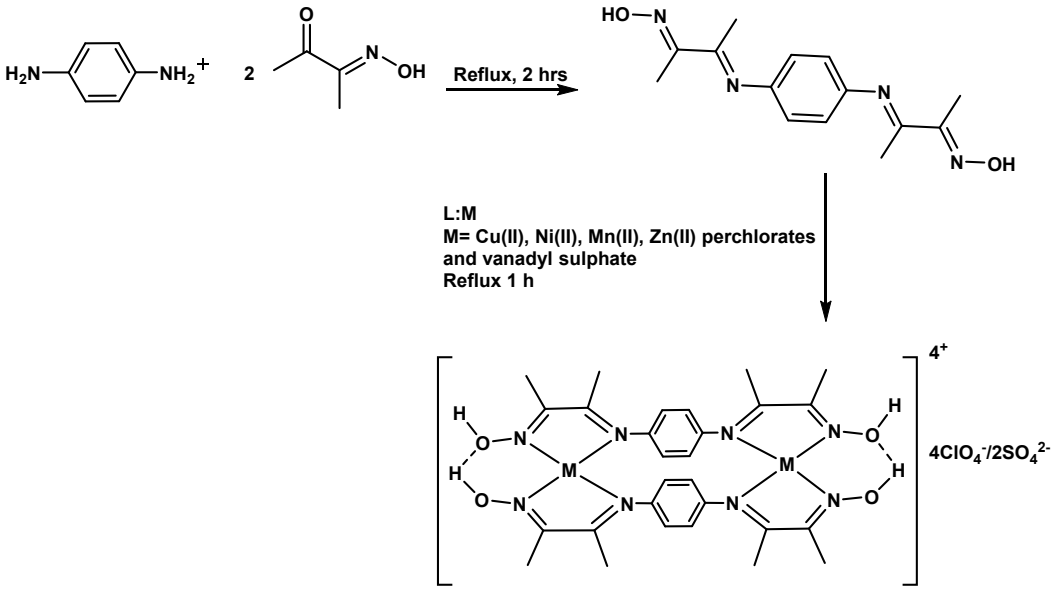

Scheme 1

This solution was poured (25 mL in each dish) into petri dishes and then allowed to attain room temperature. Wells (6 mm in diameter) were cut in the agar plates using proper sterile tubes. A blank disc was soaked in the solvent (DMSO) and implanted as negative control on each plate along with the standard drugs. Then, the wells were filled up to the surface of agar with 0.1 mL of the test compounds dissolved in DMSO (200 µg/mL). The plates were allowed to stand for an hour in order to facilitate the diffusion of the drug solution. Then the plates were incubated at 37 °C for 24 h for bacteria and 48 h for fungus and the diameter of the inhibition zones was measured [17]. Minimum inhibition concentration is the lowest concentration (MIC) of solution to inhibit the growth of a test organism and MICs were detected by the serial dilution method. The lowest concentration (µg/mL) of compound, which inhibits the growth of bacteria after 24 h incubation at 37 °C, and of fungi after 48 h incubation at 37 °C was taken as the MIC.

2.4. DNA binding experiment

The binding of complexes to CT-DNA was studied by using electronic absorbance spectral method. The concentration of CT-DNA was determined from its absorption intensity at 260 nm with molar extinction coefficient of 6600 $m^{-1}cm^{-1}$. Solutions of CT-DNA in 50 mM NaCl/50 mM Tris-HCl (pH = 7.2) gave ratio of UV absorbance at 260and 280 nm A_{260}/A_{280}= 1.8-1.9 indicating that DNA was sufficiently free of protein contaminations [18]. The absorbance spectra of copper(II) metal complex was determined by increasing the CT-DNA concentration to copper(II) metal complex in 5 mM Tris-HCl/ 50 mM NaCl buffer (pH = 7.2).

2.5. Gel electrophoresis method

DMF solutions of the complexes were placed in clean Eppendorf tubes and 1 µg of pBR322 DNA was added. The contents were incubated for 30 min at 37 °C and loaded on 0.8% Agarose gel after mixing 5 µL of loading buffer (0.25% bromophenol blue + 0.25% xylene cyanol + 30% glycerol sterilized distilled water). Electrophoresis was performed at constant voltage (100 V) until the bromophenol blue reached to the ¾ of the gel. The gel was stained for 10 min by immersing in an ethidium bromide solution [19]. The gel was then destained for 10 min by keeping in sterilized distilled water and the plasmid bands visualized by photographing the gel under a UV Transilluminator. The efficiency of DNA cleavage was measured by determining the ability of the complex to form open circular (OC) or nicked circular (NC) DNA from its super coiled (SC) form.

3. Results and discussion

3.1. Synthesis

The resulting solid compounds are intensely colored and stable in air. The ligands soluble in common organic solvents and the complexes are soluble only in DMF and DMSO. So, the single crystal could not be obtained for the obtained compounds. The elemental analysis is in good agreement with that calculated for the proposed formulas. The molar conductance of all complexes was measured in DMSO using 1×10^{-3} M solutions at room temperature. In molar conductivity studies, the values indicate that all metal complexes are electrolytic in nature (Table 1).

IR spectrum in the region of 4000-400 cm^{-1} provides useful information regarding the coordination of metal(II) complexes and are analyzed with the comparing of the ligands. The ligand H_2L_1 and H_2L_2 shows the strong band at 1620 and 1601 $cm^{-1}$are associates with the formation of C=N group. The shift in frequencies observed in metals complexes are due to coordination of nitrogen with metal ions. The appearance of new weak bands at 460-470 cm^{-1} is due to the formation of M-N. The strong band at 962 and 950 cm^{-1} are assigned to ν(V=O), this band is observed as a new peak for the complexes and are not present in the spectrum of free ligands. The presence of ionic sulphate group in vanadyl complexes are confirmed by the appearance of strong bands at 1035 and 1030 cm^{-1} [20]. The most characteristic of oxime ligand is the formation of hydrogen bond and the weak and broad band in the range of 3410 to 3320 cm^{-1} which is assigned to the formation of intra-molecular hydrogen bond between the dioxime oxygen atoms [21].

Table 1. Electronic spectral data and magnetic moment value of the ligands and its complexes.

Compounds	Molar conductance ($ohm^{-1}\cdot cm^2\cdot mol^{-1}$) in DMF	Magnetic moments μ_{eff} (B.M.)	Transitions (nm)			Tentative assignments
			π→π*	n→π*	d→d	
H_2L_1	9.0	-	240	330		
1	280	1.75	254	390	545	$^2B_{1g} \rightarrow {}^2A_{2g}$
2	270	Diamagnetic	255	380	515	$^1A_{1g} \rightarrow {}^1A_{2g}$
3	275	5.24	255	395	430	
4	270	Diamagnetic	255	390		
5	165	1.77	250	385	535	$^2B_{2g} \rightarrow {}^2E$
H_2L_2	10.0	-	250	340		
6	285	1.76	256	395	540	$^2B_{1g} \rightarrow {}^2A_{2g}$
7	273	Diamagnetic	255	390	520	$^1A_{1g} \rightarrow {}^1A_{2g}$
8	280	5.28	255	385	435	
9	278	Diamagnetic	250	390		
10	170	1.79	255	380	530	$^2B_{2g} \rightarrow {}^2E$

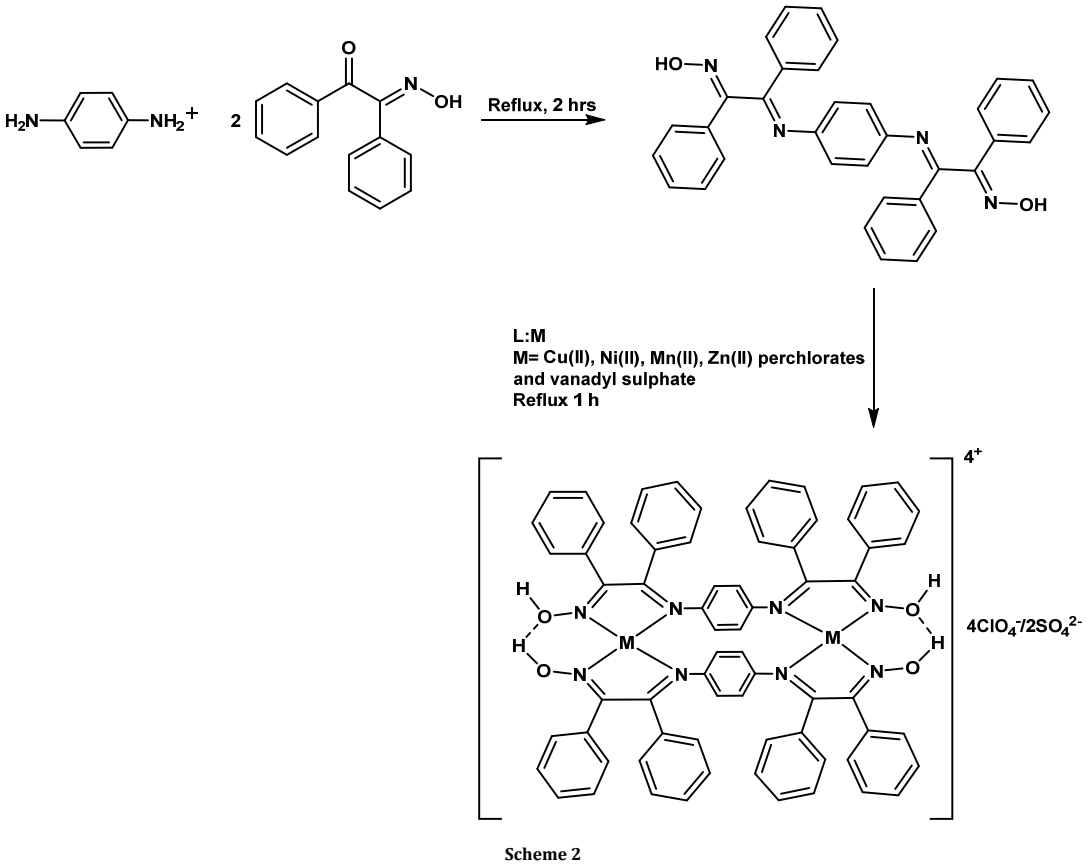

Scheme 2

3.2. Electronic, EPR spectra and magnetic moment measurements

In electronic spectrum of the Schiff base ligand (H_2L_1 and H_2L_2), absorption bands at 240,250 and 330, 340 nm assigned to π→π* and n→π* transition, respectively. These transitions are shifted towards lower frequencies, due to the coordination of the ligand with the metallic ions [22,23]. All the metal complexes exhibit an absorption band in the range 380-400 nm, which is assigned to the ligand to metal charge transfer (LMCT) transition. In the electronic spectrum of Cu(II) complexes, the presence of a new band at 545,540 nm is attributed to $^2B_{1g} \rightarrow {}^2A_{2g}$ transitions. The magnetic moment (μ_{eff}) for these complexes (**1** and **6**) are found to be 1.75 and 1.76 B.M. per copper ion are normal at room temperature indicating no direct interaction between two copper centers. These transitions as well as the measured value of the magnetic moment suggest a square planar geometry of the compound **1** and **6** (Table 1).

The nickel(II) complexes (**2** and **7**) show the absorption at 515, 520 nm are due to $^1A_{tg} \rightarrow {}^1A_{2g}$ transitions and square planar structures around nickel(II)ion in metal complexes **2** and **7**. The Mn(II) complexes (**3** and **8**) absorptions at 430, 435 nm and the magnetic moments 5.24 and 5.28 B.M. attributed to the tetrahedral structure around Mn(II) in complexes **3** and **8**. In VO(II) complexes (**5** and **10**) the absorptions at 535, 530 nm are assigned to $^2B_{2g} \rightarrow {}^2E$ transitions and the magnetic moment of 1.77 (**5**) and 1.79 (**10**) B.M. are due to square pyramidal geometry of VO in metal(II) complexes.

The X-band EPR spectra of complex **1** and **6** were recorded in the solid state at 25 °C. The spectrum of the Cu(II) complexes **1** and **6** complex exhibits $g_{\parallel}$ at 2.28, 2.25 and $g_{\perp}$ at 2.05, 2.01, respectively. The value of $g_{\parallel} > g_{\perp} > g_e$ (g_e = 2,0023) for the complexes (**1** and **6**) predicts that the unpaired electron present in the $dx^2\text{-}y^2$ of Cu(II) ion. For the complex **1** and **6** $g_{\parallel} < 2.3$, which is confirmed the covalent character of the metal-ligand bond [24,25].

Table 2. Antimicrobial activity of the Schiff base ligands and its complexes *.

Compound	Gram-positive bacteria						Gram-negative bacteria						Fungus		
	S. aureus			*B. subtilis*			*E. coli*			*K. pneumoniae*			*A. niger*		
	A	B	C	A	B	C	A	B	C	A	B	C	A	B	C
H_2L_1	9	7	5	11	9	6	9	7	5	10	7	6	10	7	3
1	20	17	14	21	18	15	20	18	16	22	18	15	14	12	10
2	18	15	12	19	17	12	19	17	14	19	16	13	13	11	9
3	17	14	12	20	17	13	18	15	13	18	15	12	13	10	8
4	16	14	11	19	16	12	17	14	11	17	14	11	12	10	7
5	18	15	13	20	17	14	18	15	13	18	15	12	13	11	6
H_2L_2	12	10	8	13	9	6	11	8	6	13	10	8	9	7	5
6	22	18	16	24	20	17	22	19	17	24	21	17	16	14	12
7	20	18	15	22	18	15	21	18	16	23	20	17	15	12	11
8	19	16	13	23	20	15	20	17	15	21	18	15	14	13	10
9	18	15	13	22	19	16	21	18	16	20	17	15	15	13	11
10	20	17	15	23	20	16	19	16	14	23	20	17	15	13	10
Ampicillin	35	30	25	34	29	26	36	31	27	35	31	26			
Fluconazole													30	26	21

* A = 150 µg/mL; B = 100 µg/mL; C = 50 µg/mL, Inhibition zone in mm.

The shape of the spectrum is consistent with the square-planar geometry around each Cu(II) centre in the complex (Figure 1 and 2).The exchange interaction between the metal center has been calculated by using the formula G= (g||−2)/(g⊥ −2) [24]. If G > 4, the exchange interaction is negligible, but G<4 indicates considerable exchange between two metal center [26]. The synthesized Cu(II) complexes (**1** and **6**) reported in this paper give the "G" values which are greater than 4 indicating the exchange interaction is absent in two metal centers.

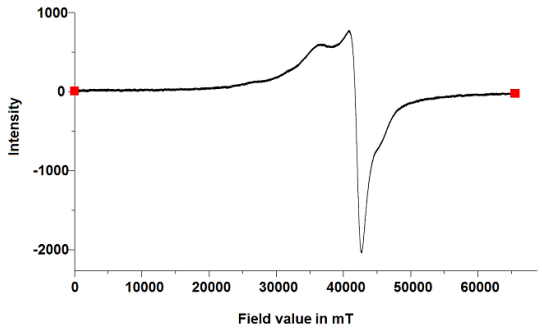

Figure 1. EPR spectra of copper(II) metal complex **1**.

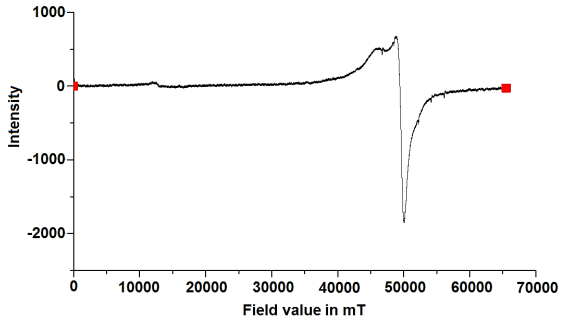

Figure 2. EPR spectra of copper(II) metal complex **6**.

The structure of ligands is confirmed by ^{1}H NMR spectra. The ^{1}H NMR spectrum of DMSO-d_6 solution of oxime ligands showed well resolved signal as expected. The spectrum of oxime ligand **1** shows singlet at δ 1.90 ppm and singlet at δ 2.60 ppm corresponding to two methyl groups. The signals between δ 7.5 to 8.5 ppm were due aromatic protons. The oxime-OH proton appears at δ 11.20 ppm. The structure of ligand was also confirmed by ^{13}C NMR spectra. The oxyimino appears at δ 156.18 ppm and imine carbon appears at δ 164.69 ppm. The peaks between δ 146 to 138 ppm are assigned to the aromatic carbons. The peak at δ 15.19 is due to methyl groups in oxime ligand. In ligand **2**, the oxime peak appears at δ 11.74 ppm in ^{1}H NMR spectra. The signals between δ 7.3 to 7.9 ppm are due to aromatic protons. In ^{13}C spectra, the imine carbon shows peak at δ 195.20 ppm and oxyimine carbon shows at δ 154.63 ppm. The peaks from δ 134 ppm to 125 ppm are assigned to aromatic carbons.

3.3. Microbial activities

The *in-vitro* biological activities of the Schiff base ligands and its metal complexes were tested against the bacteria and fungus. The organisms used in the present study are *S. aureus, B. subtilis* (as Gram-positive bacteria), *K. pneumoniae, E. coli,* (as Gram-negative bacteria) and *Aspergillus niger* as fungus. The results of the bactericidal screening of the synthesized complexes are given in Table 2. A comparative study of the ligands and their metal complexes indicates that complexes exhibit higher antimicrobial activity than the free ligands. This suggests that the chelation could facilitate the ability of a complex to cross a cell membrane and can be explained by Tweedy's chelation theory [27]. Chelation considerably reduces the polarity of the metal ion because of partial sharing of its positive charge with donor groups and possible electron delocalization over the whole chelate ring. Such a chelation could enhance the lipophilic character of the central metal atom, which subsequently favors its permeation through the lipid layer of the cell membrane. This will increase the rate of uptake and the activity of testing compounds. These complexes also disturb the respiration process of the cell and thus block the synthesis of protein, which restricts further growth of the organism. The activity of the Schiff base ligands and their metal complexes increases as the concentration increases because the concentration increases, the degree of inhibition also increases. Almost all synthesized complexes have activity against the bacteria and fungus. H_2L_1 complexes showed less microbial activity than H_2L_2 complexes, this may be due to more aromatic character of H_2L_2 complexes. Among all the metal complexes, the copper (II) complex is more active than other complexes. The variation in the effectiveness of different compounds against different organisms depends either on the impermeability of the cells of the microbes or on differences in ribosome of microbial cells [28].

3.4. DNA binding study

The absorption titration studies have been performed to monitor the mode of interaction of the complexes with CT-DNA. The absorption spectra of complex **1** (2.5×10^{-5} M) in the absence and presence of an increasing amount of CT-DNA (1×10^{-5} to 10×10^{-5} M) at room temperature in Tris-HCl/NaCl

buffer (pH = 7.2) are shown in Figure 3a. The Figure 3b shows the plot of [DNA]/(ϵ_A - ϵ_F) *vs.* [DNA] for complex **1**. The concentration of DNA is gradually increased; considerable changes were observed in the intensity of the π→π* absorption bands (254 nm) of complex **1**. The changes in the bands are hypochromicity without any red/blue shift. The result indicates that complex **1** binds to the DNA helix via non-intercalative interaction. The intercalation would lead to hypochromism and bathochromism in UV absorption spectra. Hypochromism results from the contraction of DNA in the helix axis and in hyperchromism results from the damage of DNA double helix structure. The groove binding results in structural reorganization of CT-DNA which entails partial unwinding (or) damage of double helix at the exterior phosphate bone leading to the formation of a cavity to accommodate the complex. Consequently, uptake occurs with partial melting of the double helix and generation of appropriate binding pockets [29]. In complex **6**, the same type of results was observed (Figure 4). The binding strength of metal complexes **1** and **2** are calculated by using the Equation (1).

$$[DNA]/ (e_A-e_B) = [DNA]/ (e_B-e_F) + 1/K_b (e_B-e_F) \quad (1)$$

where e_A, e_B and e_F correspond to the apparent, bound and free metal complex extinction coefficients, respectively. A plot of [DNA]/(e_A - e_F) *vs* [DNA] gave a slope of 1/ (e_B - e_F) and a Y-intercept equal to 1/K_b (e_B - e_F); K_b is the ratio of slope to the Y-intercept.

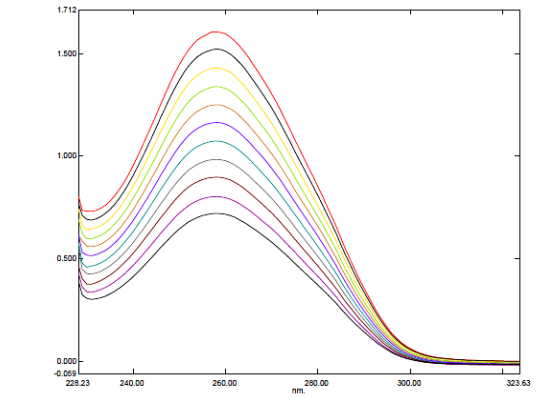

(a)

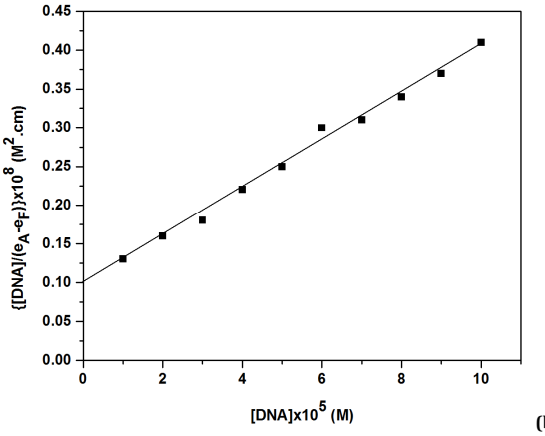

(b)

Figure 3. (a) Electronic absorption spectra of copper(II) metal complex **1** (2.5×10^{-5} M) upon the addition of CT-DNA (1×10^{-5} to 10×10^{-5} M), (b) Plots of [DNA]/e_A-e_F *versus* [DNA] for titration of CT-DNA with copper(II) metal complex **1**.

According to Equation (1), the intrinsic binding constants (K_b) were calculated to be 1.51×10^5 and 1.85×10^5 M^{-1} for complexes **1** and **6**, respectively. The values suggest that complexes **1** and **6** are strongly bind with CT-DNA. Due to the presence of more aromatic moieties in complex **6**, the binding ability is slightly higher than that of complex **1** [30,31].

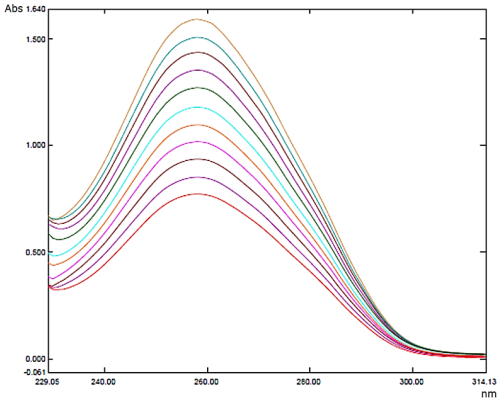

(a)

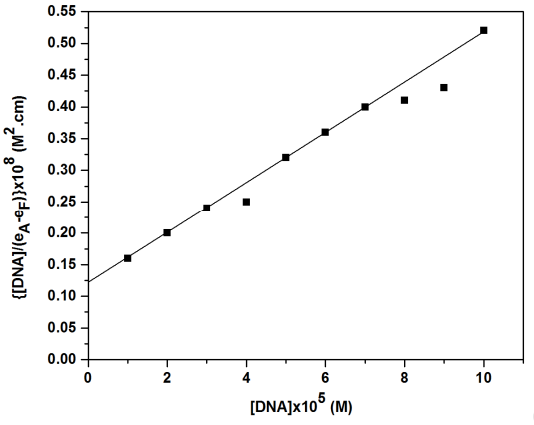

(b)

Figure 4. (a) Electronic absorption spectra of copper(II) metal complex **6** (2.5×10^{-5} M) upon the addition of CT-DNA (1×10^{-5} M to 10×10^{-5} M), (b) Plots of [DNA]/e_A-e_F *versus* [DNA] for titration of CT-DNA with copper(II) metal complex **6**.

3.5. DNA cleavage studies

The term electrophoresis describes the migration of charged particles under influence of an electrical field. Many important biological molecules, such as amino acids, peptides, proteins, nucleotides and nucleic acids, possess ionizable groups and, therefore, at any given pH, exist in solutions as electrically charged species either as cation(+) or anions(-). Under the influence of an electrical field these charged particles will migrate either to the cathode (or) to the anode, depending on the nature of their net charge [32]. When circular plasmid (pBR322) DNA is subjected to electro-phoresis, the fastest migration will be observed for super coiled form (Form I). If scission occurs on one strand (nicking), the super coiled form will relax to generate a slower moving nicked form (Form II). If both strands are cleaved, a linear form (Form III) that migrates between Forms I and II will be generated [33]. The conversion of super coiled DNA (Form I) to nicked DNA (Form II) takes place in the presence of oxidant H_2O_2. The production of hydroxyl radical as follows.

$$H_2O_2 + M^n \rightarrow M^{n+1} + {}^*OH + OH^- \quad (2)$$

These hydroxyl free radicals participate in the oxidation of the deoxyribose moiety, followed by hydrolytic cleavage of the sugar phosphate backbone. In Figure 5 and 6, the lane 1, 2 did not show any significant cleavage whereas from lane 3-7 shows the significant cleavage of DNA in presence of H_2O_2 [34].

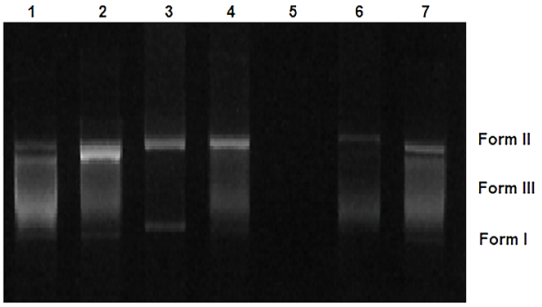

Figure 5. DNA cleavage studies of metal(II)complex (**1** to **5**). Lane 1 - pBR322 DNA - Control; Lane 2 - DNA + H_2O_2 (1 mM); Lane 3 - DNA + H_2O_2 (1 mM) + C_1 (40 µM); Lane 4 - DNA + H_2O_2 (1 mM) + C_2 (40 µM); Lane 5 - DNA + H_2O_2 (1 mM) + C_3 (40 µM); Lane 6 - DNA + H_2O_2 (1 mM) + C_4 (40 µM); Lane 7 - DNA + H_2O_2 (1 mM) + C_5 (40 µM).

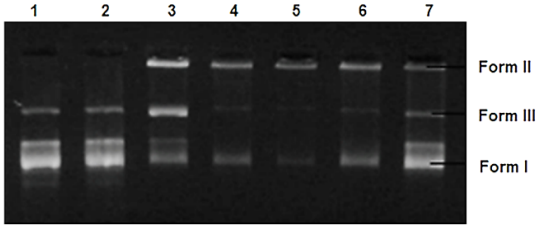

Figure 6. DNA cleavage studies of metal(II) complex (**6-10**). Lane 1 - pBR322 DNA - Control; Lane 2 - DNA + H_2O_2 (1 mM); Lane 3 - DNA + H_2O_2 (1 mM) + C_6 (40 µM); Lane 4 - DNA + H_2O_2 (1 mM) + C_7 (40 µM); Lane 5 - DNA + H_2O_2 (1 mM) + C_8 (40 µM); Lane 6 - DNA + H_2O_2 (1 mM) + C_9 (40µM); Lane 7 - DNA + H_2O_2 (1 mM) + C_{10} (40 µM).

4. Conclusions

In this work, new Schiff base and their binuclear metal complexes were designed and synthesized. The IR, UV and EPR spectral results revealed that the metal complexes Cu(II), Ni(II) have square planar geometries, VO(II) has square pyramidal geometry and Zn(II), Mn(II) have tetrahedral geometry. The ligands and theirs metal complexes were screened for their microbial activity. The result shows that all metal complexes have higher antimicrobial activity than the free ligand. The interaction of these complexes with pBR322-DNA was investigated by gel electrophoresis. All the transition metal complexes have effectively cleaved than the control pBR322-DNA.

Acknowledgements

Author Subramanian Vedanayaki is grateful to University Grant Commission, Hyderabad, India for generous financial support (MRP-5388/14 (SERO/UGC), March 2014, Com.code TNPE004).

Reference

[1]. Priyarega, S.; Senthil, R. D.; Ganesh, B. S.; Karvembu, R.; Hashimoto, T.; Endo, A.; Natarajan, K. *Polyhedron* **2012**, *34*, 143-148.
[2]. Prabu, R.; Vijayaraj, A.; Suresh, R.; Shenbhagaraman, R.; Kaviyarasan, V.; Narayanan, V. *Spectrochim. Acta A* **2011**, *78*, 601-606.
[3]. Naderi, E.; Jafari, A. H.; Ehteshamzadeh, M.; Hosseini, M. G. *Mater. Chem. Phys.* **2009**, *115*, 852-858.
[4]. Mistry, B. M.; Jauhari, S. *Res. Chem. Intermed.* **2013**, *39*, 1049-1068.
[5]. Chena, X.; Yamaguchi, A.; Namekawa, M.; Kamijoa, T.; Teramae, N.; Tong, A. *Anal. Chim. Acta* **2011**, *696*, 94-100.
[6]. Joseph, J.; Nagashri, K.; BoomadeviJanaki, G. *Eur. J. Med. Chem.* **2012**, *49*, 151-163.
[7]. Muniyandi, V.; Pravin, N.; Mitu, L.; Raman, N. *J. Mol. Struc.* **2015**, *1086*, 56-63.
[8]. Kamath, A.; Naik, K.; Netalkar, S. P.; Kokare, D. G.; Revanka, V. K. *Med. Chem. Res.* **2013**, *22*, 1948-1956.
[9]. Farag, A. M.; Guan, T. S.; Osman, H.; Abdul, M. S.; Iqbal, M. A.; Khadeer, A. M. B. *Med. Chem. Res.* **2013**, *22*, 4727-4736.
[10]. Jayaseelan, P.; Prasad, S.; Vedanayaki, S.; Rajavel, R. *Arabian J. Chem.* **2011**, DOI: 10.1016/j.arabjc.2011.07.029.
[11]. Akila, E.; Usharani, M.; Ramachandran, S.; Jayaseelan, P.; Velraj, G.; Rajavel, R. *Arabian J. Chem.* **2013**, DOI: 10.1016/j.arabjc.2013.11.031.
[12]. Chen, Z.; Zhang, J.; Zhang, S. *New J. Chem.* **2015**, *39*, 1814-1821.
[13]. Krishna, M. P.; Hussain, R. K.; Prakash, P. J.; Siddavattam, D. *Trans. Metal Chem.* **2008**, *33*, 661-668.
[14]. Mohini, Y.; Prasad, R. B. N.; Karuna, M. S. L.; Ganesh, K. C.; Poornima, M.; Sujitha P. *Med. Chem. Res.* **2013**, *22*, 4360-4366.
[15]. Sumrra, S. H.; Chohan, Z. H. *Med. Chem. Res.* **2013**, *22*, 3934-3942.
[16]. Lahiri, D.; Majumdar, R.; Patra, K.; Chakravarty, A. R. *J. Chem. Sci.* **2010**, *122(3)*, 321-333.
[17]. Joseph, J.; Nagashri, K.; Bibin, R. G. A. *J. Saudi Chem. Soc.* **2013**, *17(3)*, 285-294.
[18]. Marmur J. *J. Mole. Biol.* **1961**, *3*, 208-214.
[19]. Anbu, S.; Kamalraj, S.; Varghese, B.; Muthumary, J.; Kandaswamy, M. *Inorg. Chem.* **2012**, *51*, 5580-5592.
[20]. Shivakumar, L.; Shivaprasad, K.; Revanasiddappa, H. D. *Spectrochim. Acta A* **2012**, *97*, 659-666.
[21]. Souaya, E. R.; Hanna, W. G.; Ismail, E. H.; Milad, N. E. *Molecules* **2000**, *5(10)*, 1121-1129.
[22]. Lever, A. B. P. Inorganic electronic spectroscopy, Elsevier, Amsterdam, New York, 1984.
[23]. Sathyanarayana, E. N. Electronic absorption spectroscopy and related techniques, UniversityPress (India) limited, Hyderabad, 2001.
[24]. Kivelson, D.; Neiman, R. *J. Chem. Phys.* **1961**, *35*, 149-155.
[25]. Abdel-Aiz, A. A.; Salem, A.N.M.; Sayed, M.A.; Abolay, M.N. *Mol. Struct.* **2012**, *1010*, 130-138.
[26]. Hathaway, B. J.; Bardley, J. N.; Gillard, R. D. Essays in Chemistry, Academic Press Eds. New York, USA, 1971.
[27]. Tweedy, B. G. *Phytopathalogy* **1964**, *55*, 910-914.
[28]. Silva, C. M.; Silva, D. L.; Modolo, L. V.; Alves, R. B.; Resende, M. A.; Martins, C. V. B. Fatima, A. *J. Adv. Res.* **2011**, *2*, 1-8.
[29]. Arjmand, F.; Sayeed, F.; Muddassir, M. *J. Photochem. Photobiol. B: Biol.* **2011**, *103*, 166-179.
[30]. Iqbal, M.; Ali, S.; Rehman, Z.; Muhammad, N.; Sohail, M.; Pandarinathan, V. *J. Mol. Struc.* **2015**, *1093*, 135-143.
[31]. Sobha, S.; Mahalakshmi, R.; Raman, N. *Spectrochim. Acta A* **2012**, *92*, 175-183.
[32]. Vilson, K.; Walker, J. Principles and Techniques of Biochemistry and Molecular biology, Seventh edn., Cambridge University Press, India, 2010.
[33]. Lin, Y.; Cho, H.; Tan, L.; Yuan, Y.; Wei, W.; Ji, L. *J. Inorg. Biochem.* **2005**, *99*, 530-537.
[34]. Jayaseelan. P.; Akila, E.; Usha, R. M.; Rajavel, R. *J. Saudi Chem. Soc.* **2013**. DOI:10.1016/j.jscs.2013.07.001.